Published in final edited form as:
Curr Biol. 2011 April 26; 21(8): 681–686. doi:10.1016/j.cub.2011.03.030.

Caveolin-1 deficiency causes cholesterol dependent mitochondrial dysfunction and apoptotic susceptibility

Marta Bosch[1,*], **Montserrat Marí**[2,*], **Albert Herms**[1], **Ana Fernández**[2], **Alba Fajardo**[1], **Adam Kassan**[1], **Albert Giralt**[3,4], **Anna Colell**[2], **David Balgoma**[5], **Elisabet Barbero**[2], **Elena González-Moreno**[1], **Nuria Matias**[2], **Francesc Tebar**[1,3], **Jesús Balsinde**[5], **Marta Camps**[6], **Carlos Enrich**[1,3], **Steven P. Gross**[7], **Carmen García-Ruiz**[2], **Esther Pérez-Navarro**[3,4], **José C. Fernández-Checa**[2,8,+], and **Albert Pol**[1,9,+]

[1]Equip de Proliferació i Senyalització Cel·lular, Institut d'Investigacions Biomèdiques August Pi i Sunyer (IDIBAPS). 08036 Barcelona

[2]Departament de Mort Cel·lular i Proliferació, IDIBAPS, Consejo Superior de Investigaciones Científicas (CSIC) i Unitat d'Hepatologia, Hospital Clínic i Provincial de Barcelona, Centre d'Investigacions Biomèdiques Esther Koplowitz, CIBER de Enfermedades Hepáticas y Digestivas, 08036 Barcelona

[3]Departament de Biologia Cel·lular, Immunologia i Neurociències. Facultat de Medicina. IDIBAPS

[4]CIBER de Enfermedades Neurodegenerativas. Universitat de Barcelona. 08036 Barcelona

[5]Instituto de Biología y Genética Molecular, CSIC, 47003 Valladolid and CIBER de Diabetes y Enfermedades Metabólicas Asociadas, 08036 Barcelona

[6]Departament de Bioquímica i Biologia Molecular, Universitat de Barcelona i Institut de Recerca Biomèdica de Barcelona, Parc Científic, Barcelona

[7]Department of Developmental and Cell Biology, UC Irvine, Irvine, Ca 92697, USA

[8]Research Center for Alcoholic Liver and Pancreatic Diseases, Keck School of Medicine, University of Southern California, Los Angeles, CA 90033

[9]Institució Catalana de Recerca i Estudis Avançats (ICREA)

Abstract

Caveolins (CAV) are essential components of caveolae; plasma membrane invaginations with reduced fluidity, reflecting cholesterol accumulation [1]. CAV proteins bind cholesterol, and CAV's ability to move between cellular compartments helps control intracellular cholesterol fluxes [1–3]. In humans, CAV1 mutations result in lipodystrophy, cell transformation, and cancer [4–7]. CAV1 gene-disrupted mice exhibit cardiovascular diseases, diabetes, cancer, atherosclerosis, and pulmonary fibrosis [8, 9]. The mechanism(s) underlying these disparate effects are unknown, but our past work suggested CAV1 deficiency might alter metabolism: $CAV1^{-/-}$ mice exhibit impaired liver regeneration unless supplemented with glucose, suggesting systemic inefficiencies requiring additional metabolic intermediates [10]. Establishing a functional

[+]To whom correspondence should be addressed: checa229@yahoo.com or apols@ub.edu. Telf. 34932275400 ext3337. Fax 34934021907.
[*]These two authors have made equal contribution to this article.

link between CAV1 and metabolism would provide a unifying theme to explain these myriad pathologies [11]. Here, we demonstrate that impaired proliferation and low survival with glucose restriction is a shortcoming of CAV1 deficient cells, caused by impaired mitochondrial function. Without CAV1, free cholesterol accumulates in mitochondrial membranes, increasing membrane condensation and reducing efficiency of the respiratory chain and intrinsic anti-oxidant defence. Upon activation of oxidative phosphorylation, this promotes accumulation of reactive oxygen species resulting in cell death. We confirm that this mitochondrial dysfunction predisposes CAV1 deficient animals to mitochondrial related diseases such as steatohepatitis and neurodegeneration.

Results and Discussion

Establishing a functional link between CAV1 and metabolism would provide a unifying theme to explain the myriad pathologies resulting from CAV deficiency [11]. Thus, mouse embryonic fibroblast cells (MEFs) from *wt* and CAV1$^{-/-}$ mice [12] were treated with 2-deoxyglucose (2-DG) which inhibits glycolysis. 2-DG reduced proliferation (Figure 1A) and dramatically increased cell death of CAV1$^{-/-}$ but not *wt* MEFs (Figure 1B). Upon nutrient limitation cells rely primarily on mitochondrial OXPHOS [13]. Thus, we analysed whether the increased apoptosis in CAV1$^{-/-}$ cells upon glycolysis inhibition might be caused by increased demands on mitochondria. We treated cells with DCA to shift glucose metabolism from lactate production to OXPHOS [14] (see also Figure S1). DCA preferentially promoted apoptosis in CAV1$^{-/-}$ MEFs (Figure 1C), supporting the hypothesis that lethality is related to activation of OXPHOS. Since OXPHOS is a major source of ROS, and ROS are apoptogenic triggers, we quantified cellular ROS levels. CAV1$^{-/-}$ MEFs had a significantly higher ROS content (Figure1D), and DCA treatment enhanced ROS accumulation in CAV1$^{-/-}$ MEFs. The increased ROS was involved in the increased apoptosis, because treatment with the antioxidant BHA reduced the pro-apoptotic effect of DCA (Figure 1C). These results suggest a mitochondrial dysfunction in CAV1$^{-/-}$ cells, which is exacerbated by stimulation of OXPHOS. This sensitivity is not due to unknown additional variations in the genetic background and also occurs in the animal (see also Figures S2 and S3).

How are the CAV1$^{-/-}$ mitochondria altered? Measured by flow cytometry using Mitotracker FM (data not shown) and cellular cytochrome C content (Figures 2G and 4E), mitochondrial content is similar in both cell types. In contrast, the mitochondrial membrane potential ($\Delta\Psi$) was markedly higher in CAV1$^{-/-}$ cells (Figure 1E). The routine flux control ratio reflects how close the routine respiration operates to the respiratory capacity of the electron transport system, and was markedly higher in CAV1$^{-/-}$ cells (Figure 1F). We then purified mitochondria [15] from CAV1$^{-/-}$ and *wt* murine liver [16] and quantified function in identical environments. The fraction was enriched in cytochrome C and free of extramitochondrial contamination (Figure 1G). CAV1 was absent in *wt* mitochondria, though present in a crude fraction containing mitochondria and associated endoplasmic reticulum (ER). We determined the respiratory capacity of the purified mitochondria by examining substrate-driven oxygen consumption. The acceptor control ratio (ACR) was calculated to determine the tightness of the coupling between respiration and ATP production, and the uncoupling control ratio (UCR) calculated as the index of oligomycin-inhibited respiration and FCCP stimulated respiration. ACR was markedly lower in CAV1$^{-/-}$ mitochondria, while the UCR was unaffected (Figure 1H). Thus, CAV1$^{-/-}$ mitochondria show reduced flux between the respiratory chain and the production of energy. The apparent discrepancy of higher mitochondrial potential and higher oxygen consumption observed in CAV1$^{-/-}$ cells deserves further analysis but since the UCR is unaffected it is not caused by changes in membrane permeability.

How might CAV1 loss result in mitochondrial impairment? CAV1 contributes to intracellular cholesterol homeostasis [1–3]. CAV1 deficiency might alter mitochondrial

cholesterol levels, which regulate the organelle's function and apoptotic susceptibility [15]. CAV1$^{-/-}$ mitochondria had a significant increase (39%) in free cholesterol (Figure 2A), that could not be accounted for the presence of other cholesterol-enriched organelles (Figure 1G). This deficiency is generic: a mitochondrial fraction isolated from CAV1$^{-/-}$ MEFs had a similar increase of 33% (Figure 3A). Mass spectrometry analysis of major lipids revealed no other significant changes in the total amount of phospholipids or in the relative enrichment of each phospholipid (Table S1). Thus, only the cholesterol/phospholipid ratio was altered from 0.79 in *wt* to 1.00 in CAV1$^{-/-}$ mitochondria.

Mitochondria are cholesterol-poor organelles and little is known about regulation of their cholesterol influx/efflux [17]. Cholesterol likely reaches mitochondria through specialised ER domains called mitochondrial associated membranes (MAM) [18]. Since it is a MAM resident protein [19] and transports cholesterol from the ER to the plasma membrane [20], CAV1 could control MAM cholesterol levels. If so, CAV1 loss would influence steroid synthesis. In steroidogenic cells, after synthesis in the ER, cholesterol is transported into mitochondria and the P450 side chain cleavage enzyme (CYP11A1) converts it to pregnenolone, the steroid precursor. Mitochondrial cholesterol availability is the rate-determining step in steroid biosynthesis [21], so pregnenolone levels indicate the rate of mitochondrial cholesterol influx. Reduction of CAV1 levels in steroidogenic F2-CHO cells stably transfected with CYP11A1 caused a significant increase in pregnenolone biosynthesis (Figure 2B). Similarly, serum steroid concentrations were significantly higher in CAV1$^{-/-}$ mice (Figure 2C), confirming at the systemic level that CAV1 deficiency promotes higher mitochondrial cholesterol influx and thus increases steroid biosynthesis.

In general, cholesterol decreases membrane fluidity, so the mitochondrial cholesterol increase could alter mitochondrial membrane properties. We developed a new technique to measure mitochondrial membrane fluidity and found by di-4-ANEPPDHQ that purified CAV1$^{-/-}$ mitochondria had increased membrane condensation (Figure 2D and see supplement). Reduced membrane fluidity impairs import of glutathione into the mitochondria (mGSH) [15]. GSH is a key antioxidant that modulates the oxidative state of the cell and ultimately apoptosis [22]. Indeed, purified CAV1$^{-/-}$ hepatic mitochondria had a 28% reduction in mGSH content (Figure 2E). A mitochondrial fraction isolated from CAV1$^{-/-}$ MEFs also showed a reduction of 59% (Figure 3B). Decreased mGSH partially explains the ROS accumulation in CAV1$^{-/-}$ cells. Mitochondrial GSH reduction predisposes cells to apoptosis [15, 22] and indeed CAV1$^{-/-}$ MEFs displayed significantly higher apoptosis when challenged with TNFα (Figure 2F). The increased apoptosis was confirmed by measuring cytochrome C release into the cytosol (Figure 2G). Using cell permeable GSH ethyl ester (GSH-EE) to increase mGSH levels eliminated the difference in apoptotic sensitivity between *wt* and CAV1$^{-/-}$ fibroblasts (Figure 2F).

This data thus supports the hypothesis that CAV1 deficiency promotes cholesterol accumulation in mitochondria, reducing membrane fluidity and causing organelle dysfunction by i) reducing respiratory chain efficiency and increasing ROS levels, and ii) reducing uptake of mGSH and thus mitochondrial anti-oxidant defence. To directly test cholesterol's role, we treated purified CAV1$^{-/-}$ mitochondria with beta-cyclodextrin to extract cholesterol. This restored the cholesterol/phospholipid ratio of CAV1$^{-/-}$ mitochondria to the *wt* levels without affecting the amount of phospholipids (4.30 ± 1.15 ng cholesterol/mg protein and 6.06 ± 0.76 nmol Pi/μg protein) (Figure 2A). Critically, these CAV1$^{-/-}$ mitochondria treated with cyclodextrin had reduced membrane order as showed by di-4-ANEPPDHQ (Figure 2D) and their ACR index recovered to *wt* mitochondria levels (Figure 2H). Further, their susceptibility to mitochondrial toxins was reversed (Figure 4I). Conversely, when purified *wt* mitochondria were loaded with an additional 25% of cholesterol, they demonstrated increased membrane order (Figure 2I), reduced ACR index

(Figure 2J) and reduced entry of mGSH (Figure 2K). Re-expression by retroviral infection of CAV1 in CAV1$^{-/-}$ MEF [23], recovered mitochondrial cholesterol and mGSH levels (Figures 3A and 3B), reduced the routine flux control ratio especially after OXPHOS activation by DCA (Figure 3C), and decreased the oxidative stress caused by DCA as measured by oxidation of DHE (Figure 3D). In summary, dysfunction in the CAV1$^{-/-}$ mitochondria largely results from increased mitochondrial cholesterol.

Mitochondrial impairment should make CAV1-altered animals sensitive to diseases involving mitochondrial malfunction. Because cholesterol loading of mitochondria is known to sensitize the liver to steatohepatitis [15], CAV1$^{-/-}$ mice should be particularly sensitive to this disease. We treated mice with the agonistic anti-Fas antibody Jo2. Injury was minimal in *wt* liver but in CAV1$^{-/-}$ mice Jo2 caused appearance of serum transaminases reflecting hepatic damage (Figure 4A). Steatohepatitis progression was shown by hematoxiline/eosin and inflammatory cell infiltration of liver sections (Figures 4B and 4C). The increased susceptibility of CAV1$^{-/-}$ hepatocytes to Jo2 was reproduced in isolated primary hepatocytes (Figures 4D, 4E and 4F). Importantly, increasing cellular GSH levels by the cell permeable GSH ethyl ester rescued CAV1$^{-/-}$ hepatocytes from Jo2-induced cell death (Figure 4F).

Mitochondrial impairment and oxidative stress contribute to neuronal death in multiple forms of neurodegeneration [24], and CAV1$^{-/-}$ brain mitochondria also have increased cholesterol levels and reduced mGSH (Figures 4G and 4H), To test whether CAV1 loss also sensitized these mitochondria to typical neurodegenerative insults, we incubated mitochondria with oligomeric human recombinant Aβ1–42 (the amyloid beta peptide (Aβ) characteristic of Alzheimer's disease and a potent mitochondrial toxin [25]). CAV1$^{-/-}$ brain mitochondria had higher ROS generation (Figure 4I) and enhanced cytochrome C release (not shown). This effect was reversed by extracting mitochondrial cholesterol with cyclodextrin (Figure 4I).

Finally, we tested for mitochondrial dysfunction/sensitivity in the intact brain, by injecting 3-Nitropropionic acid (3-NP). This is a mitochondrial toxin, used extensively as a model of Huntington's disease; its toxicity is associated with oxidative stress [26]. 3-NP was injected in the striatum of *wt* and CAV1$^{-/-}$ mice and degenerating cells were visualized 24 hours later. In the CAV1$^{-/-}$ striatum we found a much larger lesion (Figure 4J) (volume quantified in serial sections) and by staining with TUNEL (Figure 4K), we calculated twice the apoptotic neurons per lesion ($62.3\times10^3 \pm 7.6\times10^3$ in *wt* and $133\times10^3 \pm 13.5\times10^3$ in CAV1$^{-/-}$, $^{**}P<0.01$).

In summary, CAV1 deficiency impairs mitochondria by promoting an increased influx and accumulation of free cholesterol in mitochondrial membranes. This increases membrane condensation, decreasing efficiency of the respiratory chain and the intrinsic anti-oxidant defence. Upon activation of OXPHOS, the combination of these factors promotes accumulation of ROS, resulting in cell death. While we only investigated the effect of the mitochondrial failure caused by CAV1 deficiency in liver, brain and fibroblasts, naturally occurring CAV1 deficiencies in humans cause disease in other tissues as well. The precise contribution of the mitochondrial dysfunction in the appearance and/or progression of the pathologies attributed to the loss of CAV should now be addressed in each specific case. In this respect, we have confirmed organismal vulnerability to mitochondrial perturbations occurring during progression of steatohepatitis and neurodegeneration. In a physiological context, cells are continuously exposed to changes in the balance between aerobic glycolysis and mitochondrial oxidative metabolism, so our findings more generally suggest that CAV deficiency will progressively result in mitochondrial failure, sustained oxidative stress, and apoptosis, casually contributing to disease pathogenesis.

Experimental Procedures

Reagents and antibodies

BHA (B1253), GSH-EE (G1404), DCA (347795), 2-DG (31060, Fluka), insulin (I9278), EGF (E1557), PDGF (P4056), EGF (E1557), collagenase type IV (C5138), glucose (8270), fatty acids (L9655) and 3-NP (N5636) were from Sigma (St. Louis, MO, USA). Jo2 (554254) was from Pharmingen (San Diego, CA, USA), Hoechst-33258, Deep Red Mitotraker (M22426), Mitotraker green FM (M-7514) and DHE (D11347) were from Molecular Probes (Eugene, OR, USA), Trypsin/EDTA from Life Technologies, TNFα (300-01A) from PeproTech (Bionova, Madrid, Spain). Monoclonal anti-cytochrome C (6H2B4) was from BD Pharmingen (San Diego, CA, USA), anti-smac/DIABLO from Calbiochem (La Jolla, CA, USA), anti-GFP (ab290) from Abcam (Cambridge, UK) and anti-CAV1 (C13630) and anti-actin from Transduction Labs (Lexington, KY, USA).

Cells and animals

MEFs [12] were grown in Dulbecco's modified Eagle's medium (DMEM) supplemented with 5% foetal bovine serum, L-glutamine (2mM), penicillin (50U/ml) and streptomycin sulfate (50μg/ml) (Biological Industries, Ltd. Israel). F2-CHO, 3T3L1 cells, $CAV1^{-/-}$-reconstituted MEFs and $CAV1^{-/-}$ MEF stably transfected with the empty vector were obtained and cultured as described [23, 27, 28]. $CAV1^{-/-}$ and *wt* mice [16] were kept under a controlled humidity and lighting schedule with a 12h dark period. All animals received human care in compliance with institutional guidelines regulated by the European Community. A complete description of the experimental procedures can be found in supplemental.

Statistical analysis

The statistical significance of differences were determined using the Student's t test, *P<0.05, **P<0.01.

Supplementary Material

Refer to Web version on PubMed Central for supplementary material.

Acknowledgments

AP is supported by grants (BFU2008-00345, CSD2009-00016 and Marató de TV3), MM (PI10/02114), AC (SAF2010-15760), FT (BFU2006-15474), CG (SAF2008-02199 and Mutua Madrileña) and CE (BFU2009-10335, CSD2009-00016) from MICINN. CE (PI040236/Marató TV3), SPG (GM64624/NIH), EP (PI071183) and JCFC (SAF2009-11417 and HI2007-0244/MCI, P50-AA-11999/NIAAA/NIH and Marató de TV3).We thanks Dr. Amèrica Giménez and Josep Mª Marimon from the Animal Facility (UB), Dr. Maria Calvo and Anna Bosch for help with confocal microscopy (SCTUB) and Maria Molinos and Susana Nuñez for technical assistance. We want to thank to Dr. Barbara Karten (Nova Scotia, Canada) for providing F2-CHO cells.

References

1. Parton RG, Simons K. The multiple faces of caveolae. Nat Rev Mol Cell Biol. 2007; 8:185–194. [PubMed: 17318224]
2. Pol A, Luetterforst R, Lindsay M, Heino S, Ikonen E, Parton RG. A caveolin dominant negative mutant associates with lipid bodies and induces intracellular cholesterol imbalance. J Cell Biol. 2001; 152:1057–1070. [PubMed: 11238460]
3. Pol A, Martin S, Fernandez MA, Ingelmo-Torres M, Ferguson C, Enrich C, Parton RG. Cholesterol and fatty acids regulate dynamic caveolin trafficking through the Golgi complex and between the cell surface and lipid bodies. Mol Biol Cell. 2005; 16:2091–2105. [PubMed: 15689493]

4. Cao H, Alston L, Ruschman J, Hegele RA. Heterozygous CAV1 frameshift mutations (MIM 601047) in patients with atypical partial lipodystrophy and hypertriglyceridemia. Lipids Health Dis. 2008; 7:3. [PubMed: 18237401]
5. Kim CA, Delepine M, Boutet E, El Mourabit H, Le Lay S, Meier M, Nemani M, Bridel E, Leite CC, Bertola DR, et al. Association of a homozygous nonsense caveolin-1 mutation with Berardinelli-Seip congenital lipodystrophy. J Clin Endocrinol Metab. 2008; 93:1129–1134. [PubMed: 18211975]
6. Lee H, Park DS, Razani B, Russell RG, Pestell RG, Lisanti MP. Caveolin-1 mutations (P132L and null) and the pathogenesis of breast cancer: caveolin-1 (P132L) behaves in a dominant-negative manner and caveolin-1 (−/−) null mice show mammary epithelial cell hyperplasia. Am J Pathol. 2002; 161:1357–1369. [PubMed: 12368209]
7. Mercier I, Jasmin JF, Pavlides S, Minetti C, Flomenberg N, Pestell RG, Frank PG, Sotgia F, Lisanti MP. Clinical and translational implications of the caveolin gene family: lessons from mouse models and human genetic disorders. Lab Invest. 2009; 89:614–623. [PubMed: 19333235]
8. Le Lay S, Kurzchalia TV. Getting rid of caveolins: Phenotypes of caveolin-deficient animals. Biochim Biophys Acta. 2005
9. Cohen AW, Hnasko R, Schubert W, Lisanti MP. Role of caveolae and caveolins in health and disease. Physiol Rev. 2004; 84:1341–1379. [PubMed: 15383654]
10. Fernandez MA, Albor C, Ingelmo-Torres M, Nixon SJ, Ferguson C, Kurzchalia T, Tebar F, Enrich C, Parton RG, Pol A. Caveolin-1 is essential for liver regeneration. Science. 2006; 313:1628–1632. [PubMed: 16973879]
11. Wallace DC, Fan W, Procaccio V. Mitochondrial energetics and therapeutics. Annu Rev Pathol. 2010; 5:297–348. [PubMed: 20078222]
12. Razani B, Engelman JA, Wang XB, Schubert W, Zhang XL, Marks CB, Macaluso F, Russell RG, Li M, Pestell RG, et al. Caveolin-1 null mice are viable but show evidence of hyperproliferative and vascular abnormalities. J Biol Chem. 2001; 276:38121–38138. [PubMed: 11457855]
13. Vander Heiden MG, Cantley LC, Thompson CB. Understanding the Warburg effect: the metabolic requirements of cell proliferation. Science. 2009; 324:1029–1033. [PubMed: 19460998]
14. Bonnet S, Archer SL, Allalunis-Turner J, Haromy A, Beaulieu C, Thompson R, Lee CT, Lopaschuk GD, Puttagunta L, Harry G, et al. A mitochondria-K+ channel axis is suppressed in cancer and its normalization promotes apoptosis and inhibits cancer growth. Cancer Cell. 2007; 11:37–51. [PubMed: 17222789]
15. Mari M, Caballero F, Colell A, Morales A, Caballeria J, Fernandez A, Enrich C, Fernandez-Checa JC, Garcia-Ruiz C. Mitochondrial free cholesterol loading sensitizes to TNF- and Fas-mediated steatohepatitis. Cell Metab. 2006; 4:185–198. [PubMed: 16950136]
16. Drab M, Verkade P, Elger M, Kasper M, Lohn M, Lauterbach B, Menne J, Lindschau C, Mende F, Luft FC, et al. Loss of caveolae, vascular dysfunction, and pulmonary defects in caveolin-1 gene-disrupted mice. Science. 2001; 293:2449–2452. [PubMed: 11498544]
17. Ikonen E. Cellular cholesterol trafficking and compartmentalization. Nat Rev Mol Cell Biol. 2008; 9:125–138. [PubMed: 18216769]
18. Hayashi T, Rizzuto R, Hajnoczky G, Su TP. MAM: more than just a housekeeper. Trends Cell Biol. 2009; 19:81–88. [PubMed: 19144519]
19. Sano R, Annunziata I, Patterson A, Moshiach S, Gomero E, Opferman J, Forte M, d'Azzo A. GM1-ganglioside accumulation at the mitochondria-associated ER membranes links ER stress to Ca(2+)-dependent mitochondrial apoptosis. Mol Cell. 2009; 36:500–511. [PubMed: 19917257]
20. Smart EJ, Ying Y, Donzell WC, Anderson RG. A role for caveolin in transport of cholesterol from endoplasmic reticulum to plasma membrane. J Biol Chem. 1996; 271:29427–29435. [PubMed: 8910609]
21. Jefcoate C. High-flux mitochondrial cholesterol trafficking, a specialized function of the adrenal cortex. J Clin Invest. 2002; 110:881–890. [PubMed: 12370263]
22. Montero J, Mari M, Colell A, Morales A, Basanez G, Garcia-Ruiz C, Fernandez-Checa JC. Cholesterol and peroxidized cardiolipin in mitochondrial membrane properties, permeabilization and cell death. Biochim Biophys Acta. 2010; 1797:1217–1224. [PubMed: 20153716]

23. Grande-Garcia A, Echarri A, de Rooij J, Alderson NB, Waterman-Storer CM, Valdivielso JM, del Pozo MA. Caveolin-1 regulates cell polarization and directional migration through Src kinase and Rho GTPases. J Cell Biol. 2007; 177:683–694. [PubMed: 17517963]

24. Lin MT, Beal MF. Mitochondrial dysfunction and oxidative stress in neurodegenerative diseases. Nature. 2006; 443:787–795. [PubMed: 17051205]

25. Querfurth HW, LaFerla FM. Alzheimer's disease. N Engl J Med. 2010; 362:329–344. [PubMed: 20107219]

26. Brouillet E, Jacquard C, Bizat N, Blum D. 3-Nitropropionic acid: a mitochondrial toxin to uncover physiopathological mechanisms underlying striatal degeneration in Huntington's disease. J Neurochem. 2005; 95:1521–1540. [PubMed: 16300642]

27. Gonzalez-Munoz E, Lopez-Iglesias C, Calvo M, Palacin M, Zorzano A, Camps M. Caveolin-1 loss-of-function accelerates GLUT4 and insulin receptor degradation in 3T3-L1 adipocytes. Endocrinology. 2009

28. Charman M, Kennedy BE, Osborne N, Karten B. MLN64 mediates egress of cholesterol from endosomes to mitochondria in the absence of functional Niemann-Pick Type C1 protein. J Lipid Res. 51:1023–1034. [PubMed: 19965586]

Highlights

1. CAV1 deficiency promotes a mitochondrial and metabolic dysfunction.
2. Without CAV1 free cholesterol accumulates in mitochondrial membranes.
3. Cholesterol increases mitochondrial membrane condensation and ROS accumulation.
4. $CAV1^{-/-}$ animals are more vulnerable to mitochondrial toxins and associated diseases.

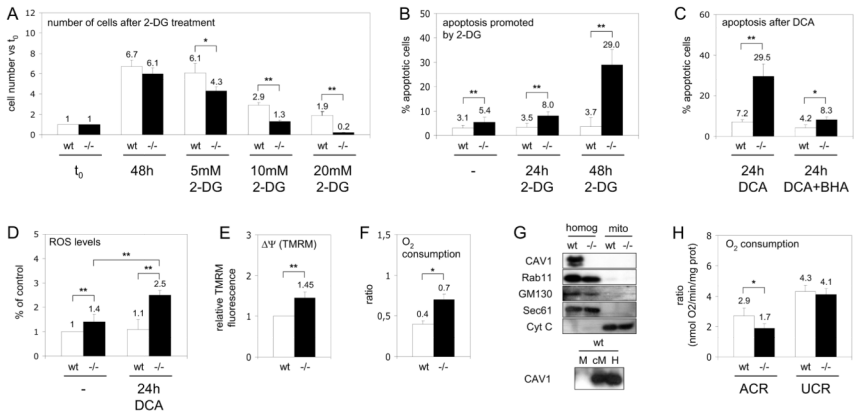

Figure 1. Mitochondrial dysfunction in CAV1$^{-/-}$ cells

(A) *Wt* (white bars) and CAV1$^{-/-}$ MEF (black bars) were cultured with 2-DG. After 48 hours cell number was determined and expressed with respect to the initial number of cells (t_0). **(B)** Apoptosis, analysed by flow cytometry via binding of annexin V and staining with propidium iodide, promoted by 5mM 2-DG. **(C)** Apoptosis promoted by DCA, some cells were pre-treated with the antioxidant BHA. **(D)** Levels of ROS in cells incubated during 24 hours with DCA. The results are expressed as the relative H2DCFDA fluorescence with respect to untreated *wt* cells. **(E)** ΔΨ m of CAV1$^{-/-}$ with respect to *wt* MEF. **(F)** Oxygen consumption by *wt* and CAV1$^{-/-}$ MEF expressed as the routine flux control ratio. **(G)** Western blotting analysis of CAV1 (plasma membrane), Rab11 (recycling endosomes), GM130 (Golgi complex), Sec61 (ER) and cytochrome C (Cyt C, mitochondria) in purified *wt* and CAV1$^{-/-}$ mitochondria (M), homogenates (H) and in a crude fraction that contains mitochondria and associated ER (cM). **(H)** Ratios of oxygen consumption in *wt* (white bars) and CAV1$^{-/-}$ mitochondria (black bars) purified from mice liver. Statistical significances were determined in at least 5 independent experiments or 10 mice using the Student's t test, *P<0.05, **P<0.01.

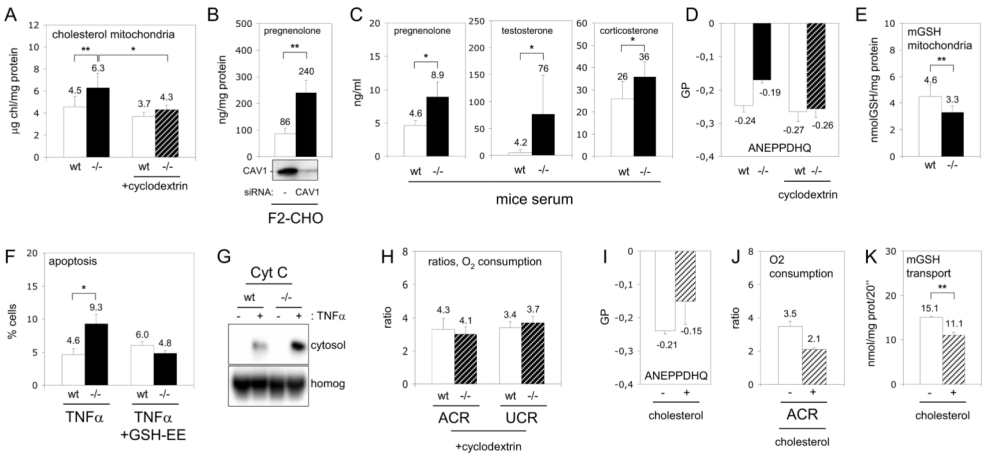

Figure 2. Cholesterol accumulation promotes dysfunction of CAV1$^{-/-}$ mitochondria

(A) Free cholesterol in *wt* (white bars) and CAV1$^{-/-}$ (black bars) mitochondria purified from mice liver. In some experiments mitochondria were pre-treated with cyclodextrin to extract cholesterol (slashed bars). (**B**) Expression of CAV1 in F2-CHO cells was reduced by RNA interference during 48 hours (Western blotting of CAV1 is shown in the bottom) and production of pregnenolone was measured during the next 24 hours. (**C**) Pregnenolone, corticosterone and testosterone levels in the serum of CAV1$^{-/-}$ (black bars) and *wt* mice (white bars). **(D)** Membrane order analysed with ANEPPDHQ of *wt* (white bars), CAV1$^{-/-}$ (black bars) and cyclodextrin-treated *wt* white bars) and CAV1$^{-/-}$ purified mitochondria (slashed bars). **(E)** Mitochondrial GSH in *wt* (white bars) and CAV1$^{-/-}$ (black bars) mitochondria purified from mice liver. **(F)** Apoptosis promoted by 24 hours of TNFα in untreated *wt* (white bars) and CAV1$^{-/-}$ MEF (black bars) or in cells treated with GSH-EE. **(G)** Cytochrome C (Cyt C) in cytosolic supernatants and homogenates (homog) corresponding to TNFα treated MEFs. **(H)** Purified mitochondria from *wt* (with bars) and CAV1$^{-/-}$ (slashed bars) were treated with cyclodextrin and the rates of oxygen consumption measured. **(I–J)** Purified *wt* mitochondria (white bars) were enriched with 25% of cholesterol (slashed bars) and membrane condensation (I) and rates of oxygen consumption (J) were measured. **(K)** Influx of a radio-labelled GSH into *wt* mitochondria untreated (white bars) or enriched with 25% of cholesterol (slashed bars).

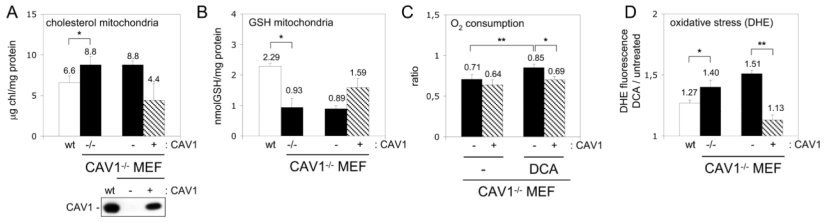

Figure 3. Re-expression of CAV1 recovers mitochondrial function

(A and B) Free cholesterol and GSH in mitochondria purified from *wt* (white bars), $CAV1^{-/-}$ (black bars), $CAV1^{-/-}$-reconstituted MEFs (slashed bars) and $CAV1^{-/-}$ MEF infected with an empty vector (black bars). CAV1 levels are shown by Western blotting. **(C)** Routine flux control ratio in untreated MEFs and in cells incubated with DCA for 5 hours. **(D)** Oxidative stress caused by mitochondrial function in MEFs. Results are expressed as the ratio between the fluorescence intensity of DHE after treating the cells with DCA for 5 hours with respect to the initial intensity.

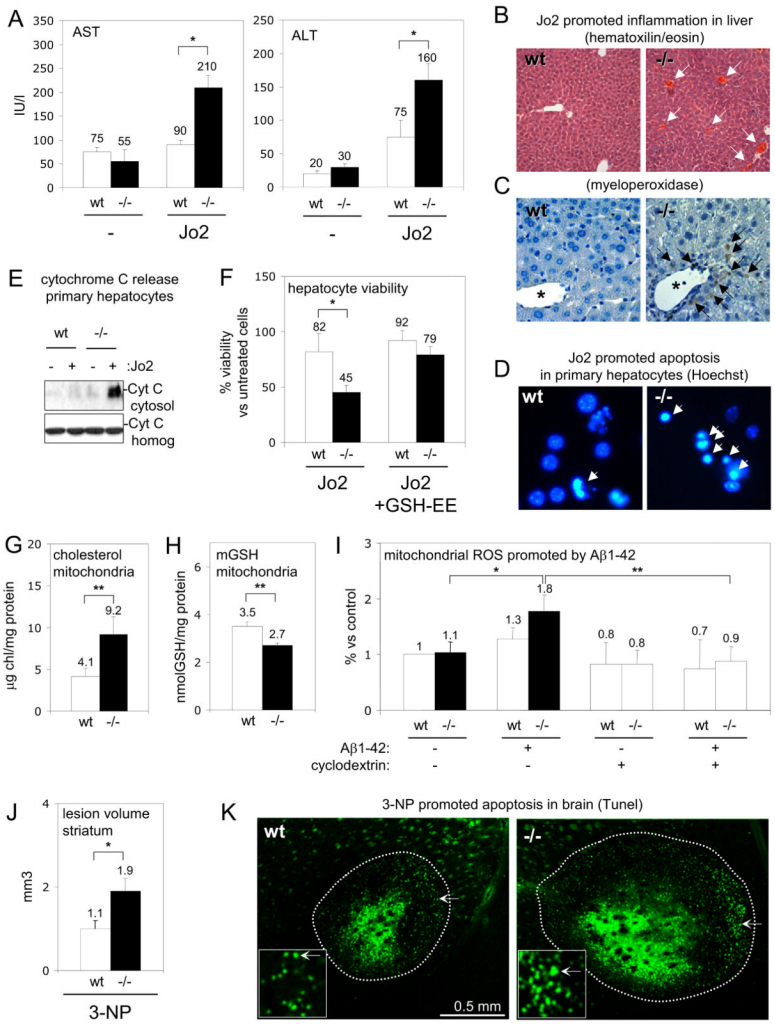

Figure 4. Dysfunction of CAV1$^{-/-}$ mitochondria enhances pathogenesis

(**A–C**) To model steatohepatitis *wt* (white bars) and CAV1$^{-/-}$ mice (black bars) were treated with Jo2. Liver damage was evaluated 24 hours later by appearance of transaminases in serum (AST and ALT). Inflammation was visualised in liver sections of *wt* (left) and CAV1$^{-/-}$ mice (right) with hematoxiline/eosin and myeloperoxidase staining. **(D–E)** W*t* and CAV1$^{-/-}$ primary hepatocytes were treated with Jo2 for 24 hours. Apoptosis in *wt* (left panel) and CAV1$^{-/-}$ hepatocytes (right) was visualized with a Hoechst staining (D) and released cytochrome C (CytC) into the cytosol quantified by Western blot (E). **(F)** MTT cell viability assay of *wt* and CAV1$^{-/-}$ hepatocytes treated with Jo2 or with Jo2/GSH-EE. (**G–H**) Free cholesterol and mGSH in *wt* (white bars) and CAV1$^{-/-}$ (black bars) purified brain mitochondria. **(I)** ROS generation in *wt* (white bars) and CAV1$^{-/-}$ (black bars) purified brain mitochondria (some treated with cyclodextrin, slashed bars) incubated with Aβ1–42. (**J–K**) 3-NP was injected in the striatum of *wt* and CAV1$^{-/-}$ mice and the volume of the lesion measured 24 hours later in serial Fluoro-Jade-stained sections and apoptotic nucleus were visualised in TUNEL-stained sections (K) of *wt* (left) and CAV1$^{-/-}$ striatum (right).